A Supersonic Intake Control System for the External Compression Mode

R. G. SCHWEIKHARDT* AND R. P. GRIPPE†
The Boeing Company, Seattle, Washington

A $\frac{1}{4}$-scale model of an early SST axisymmetric intake configuration was tested with a J85 engine and a cold pipe for the development of a bypass door control system at Mach numbers between 0.6 and 1.5. Pressure signals originating at the intake throat were used to control a system of bypass doors to maintain a constant throat Mach number while the flow through the engine or cold pipe was varied to simulate rapid throttle bursts and chops. The intake was instrumented to obtain dynamic performance information. Results indicate that the control system functioned well in maintaining the compressor face conditions within acceptable limits for relatively severe transient disturbances.

Nomenclature

A_{BY} = bypass area
A_{LIP} = lip area
dB = decibel
M = Mach number
M_L = local Mach number
M_{TH} = throat Mach number
$N/\theta^{1/2}$ = corrected engine rpm
P_{CB} = throat Mach number control signal
$PR1$ = control system reference pressure ratio (setpoint)
$PR2$ = buzz-avoidance reference pressure ratio
P_{TNS} = throat total pressure
P_{TO} = freestream total pressure
P_{T2} = engine face total pressure
P_{T3} = total pressure at compressor exit plane
S = Laplace operator
T_{TO} = freestream total temperature
W_{2c} = engine-corrected weight flow
α = intake angle of incidence
Δ = small change
ϵ = error signal

I. Introduction

THE SST uses an axisymmetric variable-geometry intake to obtain high propulsion system performance and stable operation. Variable-geometry components include a translating centerbody, movable throat doors, and variable-area bypass doors. Operation of each of these components is managed by the intake control system, which uses a closed-loop control system to maintain optimal intake performance during all airplane operating conditions and atmospheric disturbances. Efficient intake operation requires this system to operate in several different modes during various segments of the flight.

At flight Mach numbers between 0.8 and 1.8, the intake is operated in an external compression mode where airflow within the intake is entirely subsonic. This mode has been established to match intake-engine airflow requirements and to optimize the propulsion system performance. The intake centerbody is commanded to a fixed position, the cowl throat doors are opened, and the bypass doors are controlled to regulate the flow through the intake during this mode. The intake and bypass door control system must be designed to supply normal engine airflow demands with minimum drag. In addition, the control system must maintain stable and high-performance conditions at the engine compressor face over a wide range of operating conditions, including flow transients induced by the engine or the environment.

The intake throat Mach number, determined by the ratio of static to total pressure at the throat, is the bypass door control parameter. This pressure ratio is compared to a reference level (designated as the control signal set-point) to generate an error signal that is used to modulate the bypass door position and thereby maintain the desired airflow through the intake.

Development of the bypass door control system has involved a wide spectrum of technical disciplines such as unsteady flow analysis, control system analysis and design, and wind-tunnel testing techniques. The validity of the approach to bypass door control was demonstrated by the wind-tunnel test described below.

II. Description of Test Models and Facilities

Wind-tunnel tests on two small-scale axisymmetric intakes provided data for the preliminary design of the bypass door control system. Initial design information was obtained from a $\frac{1}{10}$-scale (6.36-in. lip diameter) intake model attached to a cold pipe equipped with a variable-area plug valve to simulate engine weight flow changes.

These tests were followed by construction of a $\frac{1}{4}$-scale (16.28-in. lip diameter) intake model with internal contours identical to those of the $\frac{1}{10}$-scale model. This model incorporated a variable-position bypass door system, a translating centerbody, variable-position throat doors, centerbody and cowl bleed systems, and vortex generators mounted on the centerbody. A schematic of the intake showing pressure instrumentation is shown in Fig. 1. The bypass door control signals were sensed by the static taps and total pressure probes noted in the drawing. These pressure taps and probes were connected by pneumatic lines (30-in. long) to thin-film-type strain gage pressure transducers.

The $\frac{1}{4}$-scale model was tested while fitted to either a cold pipe or a J85 engine. The installed intake-engine combination is shown in Fig. 2. Sinusoidal duct pressure variations, used to determine intake duct frequency response, were generated by a removable rotating-ring discrete frequency pulsator attached to the rear of the intake. This device is also shown in Fig. 2.

Presented as Paper 70-695 at the AIAA 6th Propulsion Joint Specialist Conference, San Diego, Calif., June 15–19, 1970; submitted September 17, 1970; revision received April 29, 1971. The authors wish to express their appreciation to Dr. K. S. Chun for his support and comments.

Index category: Subsonic and Supersonic Airbreathing Propulsion.

* Research Engineer, Propulsion Staff; presently graduate student, University of Chicago. Member AIAA.

† Research Engineer, Aircraft Noise Research Unit.

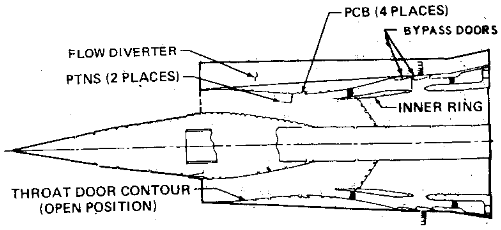

Fig. 1 Intake instrumentation.

The $\frac{1}{4}$-scale intake model was tested in the 16- by 16-ft transonic propulsion wind tunnel (PWT-16T) at Arnold Engineering and Development Center (AEDC), Arnold Air Force Station, Tullahoma, Tennessee. Steady-state and closed-loop control system tests were conducted at tunnel Mach numbers of 0.6, 0.9, 1.35, and 1.5 and intake angles of attack of 0 and 8 deg. Disturbances to the controlled intake were weight flow changes generated by exit plug transients and engine power setting transients. During the closed-loop intake testing, selected control system parameters were displayed online by optical oscillograph recorders and Brush strip chart recorders. Permanent dynamic data were recorded on a Vidar tape recording system.

III. Analysis of Steady-State Data

Criteria

An analysis of the steady-state data taken with the intake operating in the external compression mode is necessary to provide information on the intake characteristics affecting the control system. It also establishes a basis for determining the control system setpoint. The requirements to maintain stable intake operation, high intake performance, and stable intake control provide a set of criteria and a basis for identifying intake characteristics most important to the control system and for establishing the intake control system setpoint. Specifically, steady-state analysis must provide the range of stable intake weight flows, the intake performance characteristics within this range, and the intake control signal characteristics.

The upper limit on throat Mach number (i.e., intake weight flow) is determined primarily by intake performance and engine stall characteristics. The trends of compressor face distortion representative of the test results are shown schematically in Fig. 3a (for experimental curves, see Fig. 7). This curve shape is characteristic of all cases where the throat area is too small to allow the intake to start. The knee of the curve coincides with the onset of intake choking. To the left of the knee, the distortion level is low, but to the right, the distortion rises rapidly to values that exceed the engine stall limit. Intake pressure recovery curves, sketched in Fig. 3b, show a similar shape except that to the right of the knee the recovery rapidly decreases.

The knee of the distortion curve has been used to establish the upper limit on intake throat Mach number so that small perturbations in throat Mach number do not cause the distortion to exceed the engine stall limit. The locus of throat Mach numbers that permit premature intake starting establishes the remaining portion of the upper throat Mach number boundary.

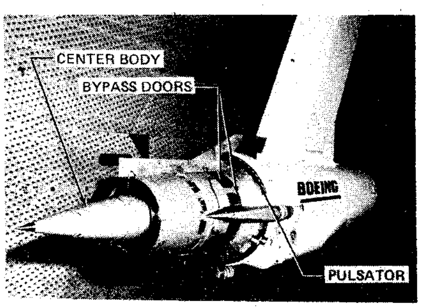

Fig. 2 Installed intake.

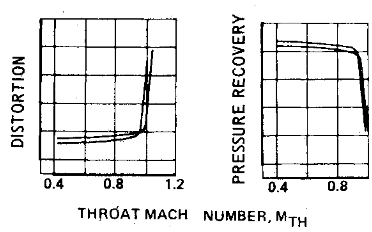

Fig. 3 Intake performance.

Intake buzz establishes a portion of the lower throat Mach number operating boundary. Identification of this boundary is the first requirement for defining the external compression operating boundaries. The remaining portion of the lower operating boundary is defined by spillage drag and internal flow separation considerations.

Figure 4 shows the boundaries of stable intake weight flows for the external compression Mach number range.

The intake performance and control signal characteristics within the operating range thus defined are necessary to establish a control system set-point. When intake pressure recovery and distortion are relatively constant over the range for stable operation as shown in Fig. 3, selection of the control system setpoint is governed by 1) intake spillage drag, 2) magnitude and uniformity of the steady-state control signal gain, and 3) control system tolerances.

The setpoint schedule that follows the upper operating boundary would maintain the maximum possible intake weight flow and hence minimize the spillage drag. However, scheduling the setpoint in this manner increases over-all system complexity. This complexity could be reduced by selecting a single setpoint value for the entire control mode. But this fixed setpoint control scheme will increase the spillage drag at the lower freestream Mach numbers. Trade studies have shown the single setpoint scheme to be superior to the schedule for the SST application.

Experimental Results

The external compression mode buzz boundaries determined experimentally with the $\frac{1}{10}$- and $\frac{1}{4}$-scale models are shown in Fig. 5. Analytical determination of these boundaries is not practical because the buzz-initiating mechanisms are dependent on normal shock-boundary layer interactions and vortex sheets. The $\frac{1}{4}$-scale data show the buzz boundary changes associated with cold pipe and engine operation and the effects of intake angle of attack; the $\frac{1}{10}$-scale data provide a comparison to determine scaling effects and to extend the information to the limit of the external compression range.

The data indicate that the incipient buzz boundary with cold pipe varies between throat Mach numbers of 0.56 and 0.68 over the freestream Mach number range from 1.3 to 1.8. Intake angle-of-attack operation reduced both the range of stable throat Mach numbers and the buzz-free supersonic freestream Mach number range. Buzz was encountered at Mach numbers as low as 1.1 and at throat Mach numbers as high as 0.80 for the 8° angle-of-attack case. The stable throat

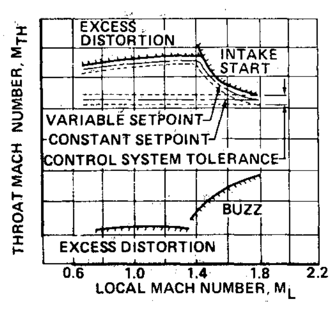

Fig. 4 Operating limits.

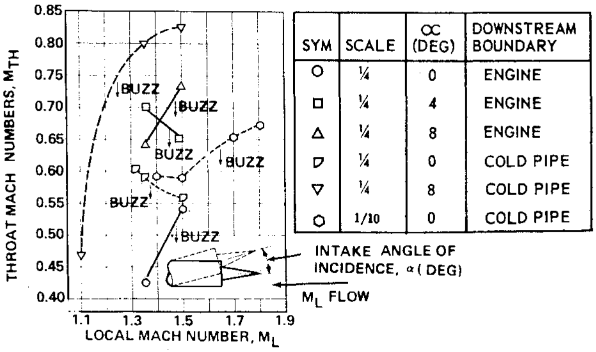

Fig. 5 External compression mode buzz limits, ¼-scale data.

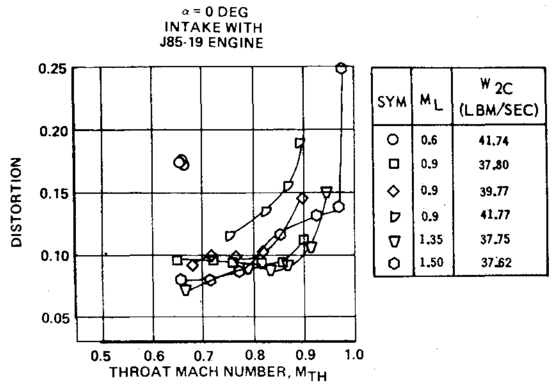

Fig. 7 External compression intake distortion, ¼-scale data.

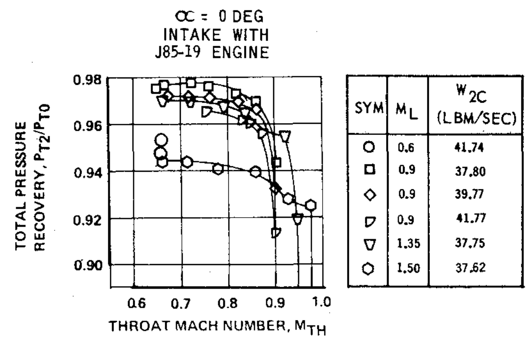

Fig. 8 External compression pressure recovery, ¼-scale data.

Mach number operating range was decreased about 0.04 for each degree of angle of attack. These data suggest that throat Mach number scheduling with angle of attack may be required.

Exchanging the cold pipe for the engine increased the range of stable throat Mach numbers, a result previously reported by Conners.[1] This is indicated in Figure 5 by the 0- and 8-deg angle-of-attack cases. These increased operating limits were used for all closed-loop testing with the engine.

The loci of the breakpoints of the experimental distortion curves, defined as the upper limit on throat Mach number, are shown in Fig. 6. These curves were derived from the performance curves of Figs. 7 and 8. All breakpoints occurred above a throat Mach number of 0.80, indicating this value is a reasonable upper bound. The variation in breakpoint at a given freestream Mach number was caused by the variation of the flow path of the air leaving the intake. Increasing the bypass door flow rate normally decreased the level of distortion and the distortion gradient with respect to throat Mach number.

The experimentally determined starting throat Mach numbers for the $\frac{1}{10}$- and ¼-scale models are shown as the "intake started" boundary in Fig. 9. The $\frac{1}{10}$-scale data were used to extrapolate the ¼-scale intake-engine data to Mach numbers beyond 1.5.

Other experimentally determined intake operating limits as defined by ¼-scale tests at 0° angle-of-attack are also presented in Fig. 9. The dashed lines indicate projected values based on $\frac{1}{10}$-scale cold pipe results. Lines of constant distortion level are added for reference. These boundaries define the throat Mach number range admissable for closed-loop operation. Final selection of the setpoint depends on the intake control signal gains associated with the setpoint.

Figure 10 shows the external compression control signals obtained from the ¼-scale intake-engine combination. The slope or gain, $\Delta(P_{CB}/P_{TNS})/\Delta(A_{BY}/A_{LIP})$, of these signals and the sloping portion of the curves are of primary importance. The principal factor affecting the closed-loop control system stability is the variation of control signal gain.

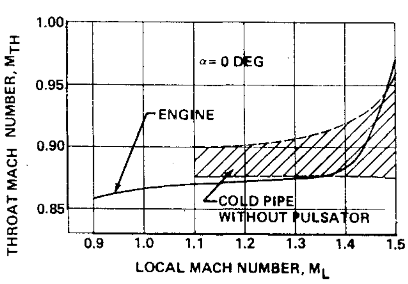

Fig. 6 External compression distortion breakpoint loci, ¼-scale data.

Knowledge of these characteristics of the control signal gain is thus required for determining the control loop gain. The sloping portion of the curve establishes the bypass door position range over which effective throat Mach number control can be maintained.

The control signals at freestream Mach numbers of 0.9, 1.35, and 1.5 displayed relatively uniform characteristics. The signal gains are relatively constant through the midsections of the curves, with decreases appearing at both ends. The apparent lack of bypass door effectiveness at a freestream Mach number of 0.6 is a result of either intake choking, sharp lip separation, lack of bypass door pressure differential, or bleed system flow reversal. Intake development should eliminate these problems.

Gain change as a function of bypass door position, for a constant control signal value, is the most interesting phenomenon since it represents control signal gain variations under actual control system operating conditions. Control signal gain as a function of bypass door position is plotted in Fig. 11. The plot indicates gain changes as large as three to four times the minimum value. It is desirable to select a control system setpoint that minimizes the gain variation and simultaneously minimizes spillage drag. Although the data shown are for a single setpoint value $M_{TH} = 0.81$, the gain variations are relatively similar for the operating range of throat Mach

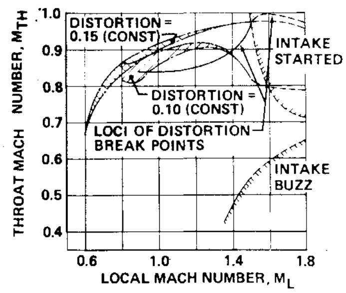

Fig. 9 Intake operating limits with engine, ¼-scale data.

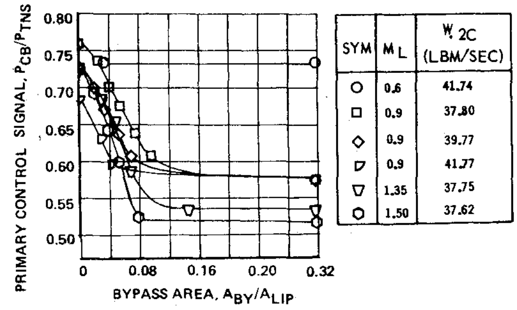

Fig. 10 External compression primary control signals, ¼-scale data.

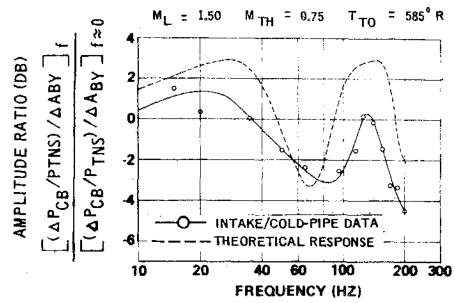

Fig. 12 Response of control signal pressure ratio, P_{CB}/P_{TNS}, to pulsator sweep.

numbers. Allowance for the large gain variations, therefore, had to be incorporated into the control system design.

IV. External Compression Duct Dynamics

During closed-loop operation, the bypass doors respond to variations in the control signal pressure ratio such that the Mach number at the throat is head nearly constant. The relation between the control signal pressure ratio P_{CB}/P_{TNS} and the bypass door opening A_{BY} is important in over-all control loop operation.

The dynamic relationship between the control signal pressure ratio and the area of the bypass door opening can be represented by a transfer function. This function is normally obtained by operating the intake in a wind tunnel and measuring the response of the control signal in response to bypass door excitation. In the current test, a rotating ring pulsator device was used to obtain the intake response for frequencies up to 250 Hz; the bypass doors cannot provide oscillatory disturbances beyond 30 Hz.

During the test period, 21 pulsator frequency sweep runs were made. Nine of these runs were made with the J-85 engine and 12 with the cold pipe.

A typical control signal response with the intake-cold pipe configuration is shown in Fig. 12. Figure 12 also shows the theoretical response based on a mathematical model of the duct, developed using the small-perturbation theory similar to that employed by Ross Willoh.[2] Theoretical predictions of the control signal response were essential to the design and simulation work that preceded the test.

V. Closed-Loop Intake Control

A block diagram of the ¼-scale intake bypass door control system is shown in Fig. 13. This system is composed of three major elements: 1) six pressure transducers that provide four electrical signals for P_{cb} and two signals for P_{tns} to an analog computer; 2) provision for manual actuation of the bypass doors; 3) a door actuation system composed of a servocontroller, hydraulic servovalve, hydraulic actuator, and position feedback transducer. An analog computer operates on the four P_{CB} signals and the two P_{TNS} signals to yield the control signal P_{CB}/P_{TNS}; forms the error signal ϵ by comparing this ratio to a reference pressure ratio signal; and provides the necessary outer loop gain and integration function for achieving over-all loop stability and performance.

The ¼-scale intake bypass door system was operated under closed-loop control at local Mach numbers M_L from 0.9 to 1.5. Flow transients were generated through manual control of the exit plug position with the intake-cold pipe configuration and through manual operation of the engine power level for the intake-engine configuration. Closed-loop operation at Mach 0.6 was not attempted due to the poor control signal gain characteristics exhibited at this condition during steady-state testing (Fig. 10).

A typical bypass door response to an exit plug transient is shown in Fig. 14. In this case the plug position history produced a corrected weight flow transient of approximately 20 lbm/sec². This is equivalent to a weight flow transient of almost 50% per sec, a rate considerably in excess of the maximum an SST might encounter during flight.

Figure 14 also shows the operation of the position coordination feedback loop shown in the control system block diagram. During normal closed-loop operation, the position coordination loop behaves as an open circuit and has no effect on the control system operation. However, if a sufficiently large change in weight flow is encountered, the bypass doors will be driven to either a fully open or a fully closed position. When this happens, the position coordination loop limits the servovalve current to a safe value and allows the system to recover more rapidly.

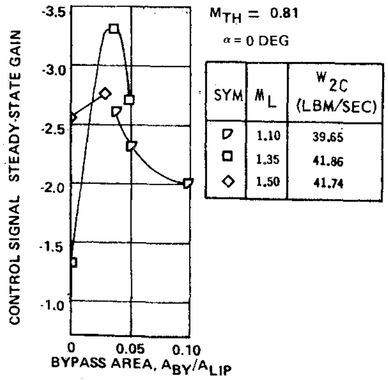

Fig. 11 External compression steady-state duct gain, ¼-scale data.

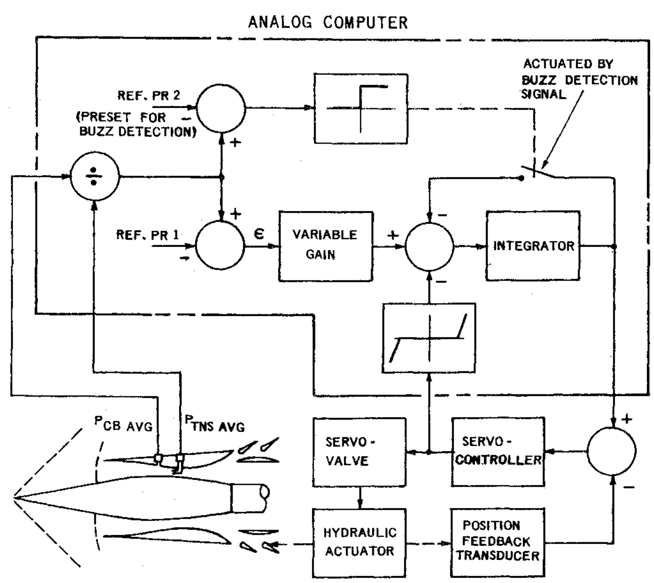

Fig. 13 Bypass door control system for external compression mode.

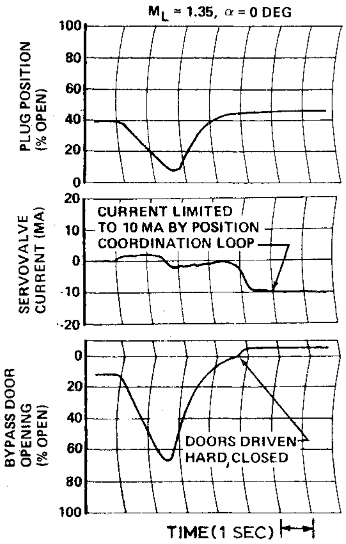

Fig. 14 Close-loop response of intake cold-pipe configuration.

The closed-loop bypass door control system was tested with the intake-engine combination at Mach numbers of 1.35 and 1.5. Extracts of the strip recorder data for the case of a throttle burst followed by a throttle chop are shown in Fig. 15. These data include time histories for engine-corrected weight flow obtained continuously from an analog computer that processed the outputs from four static pressure and two total pressure probes located at the compressor face. An independent hand computation was made using the J-85 engine compressor map and the time histories for engine rpm and compressor pressure ratio. The calculated weight flow, shown by broken lines superimposed on the data trace, compares reasonably well with the measured data.

These weight flow histories show that the maximum rate of weight flow change $\partial W_{2c}/\partial t$ is approximately 25 lbm/sec^2. The maximum change in the control signal pressure ratio from the setpoint reference value during the input transients shown in Fig. 15 is ± 0.045. This implies that during these transients the bypass door loop effectively maintained the throat Mach number at 0.74 ± 0.07. In addition, the average total pressure at the compressor face $P_{T2_{AVG}}$ was essentially unaffected by the transient. Considering the high weight flow rates to which the intake was subjected, it can be concluded that the control loop performed very satisfactorily.

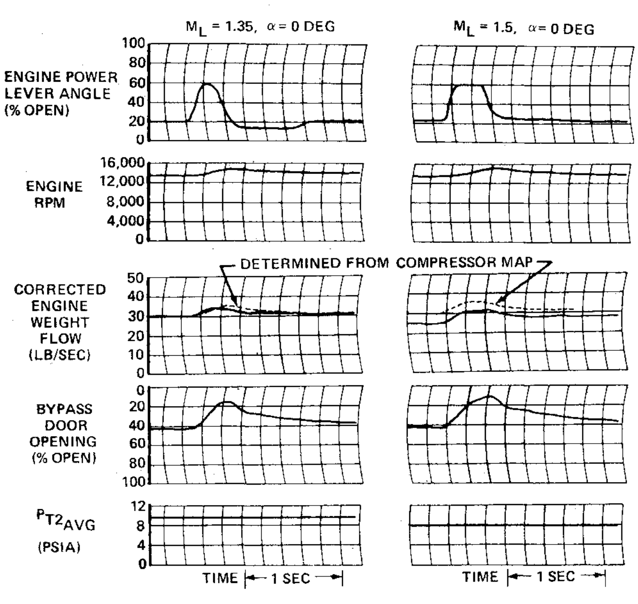

Fig. 15 Closed-loop response to throttle burst-chop transient.

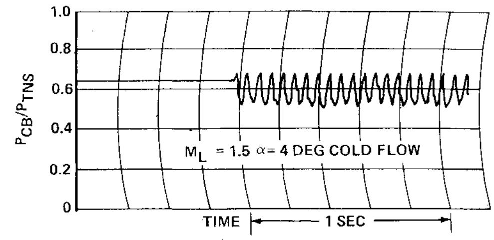

Fig. 16 Control signal pressure ratio time histories during buzz.

Application of Bypass Loop to Intake Buzz Avoidance

At Mach numbers above approximately 1.1, intake buzz is possible, depending on the angle-of-attack and the throat Mach number. During the test program, buzz was intentionally induced many times. Buzz duration for the intake-engine combination was limited to avoid possible damage to the engine.

Because of the potential damaging effects of this phenomenon, tests were conducted to determine an automatic method of detecting or avoiding buzz for implementation on an SST prototype. One technique that partially accomplished this objective is as follows.

At each Mach number and intake angle of incidence investigated during the steady-state test period, the critical throat Mach number, below which the intake will buzz, was determined. It follows that whenever the corresponding value for the P_{CB}/P_{TNS} control signal is exceeded, the intake will buzz. By setting the reference level of $PR2$ (shown in Fig. 13) at a value slightly below this threshold and the value of $PR1$ at a safe nonbuzz level, the relay across the control system integrator will automatically open, thereby closing the loop, whenever the $PR2$ threshold is exceeded. With the control loop thus closed, the control system will override all manual inputs and rapidly bring the throat Mach number back to the value set by $PR1$.

During the test, it was found that if reference level $PR2$ was not carefully determined and set, the intake would buzz before this level is reached. When buzz occurred, the average value of P_{CB}/P_{TNS}, as shown in Fig. 16, invariably fell below the value that existed prior to buzz. As a result, the peaks of the oscillating P_{CB}/P_{TNS} signal were often too low to trigger the closed-loop control system. The intake therefore continued to buzz until the flow through the intake was increased by some other means.

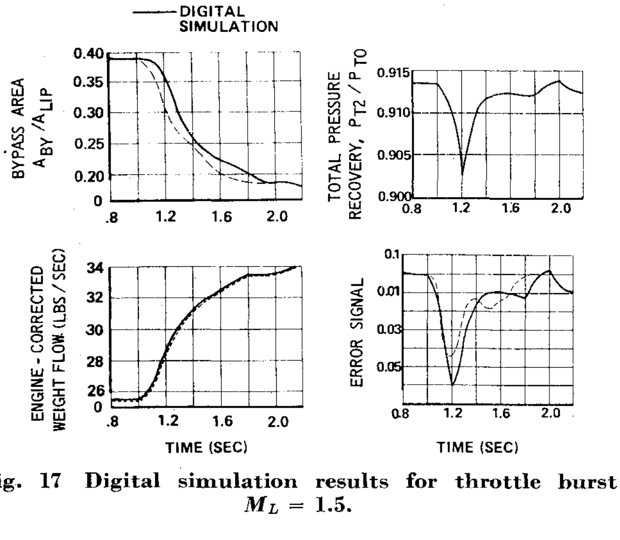

Fig. 17 Digital simulation results for throttle burst $M_L = 1.5$.

Comparison with Simulation Results

A digital computer simulation of the intake-engine configuration with bypass door control has been developed for the external compression mode. The validity of this simulation was established by comparing the actual and simulation responses to a throttle burst imposed during the closed-loop test phase. These data are compared in Fig. 17. The computer pressure recovery at the compressor face was not compared with actual data due to a lack of sufficient resolution on the strip chart record for $P_{T2_{AVG}}$. However, the good agreement shown for the other parameters attests to the overall integrity of the sumulation.

VI. Conclusions

Several conclusions can be drawn from the information obtained through the various steady-state and open- and closed-loop tests conducted on the $\frac{1}{4}$-scale intake model.

The experimentally determined steady-state operating boundaries indicated a constant control system setpoint could be used to maintain stable, high-performance intake operation during external compression. The steady-state control signal characteristics were used to establish the gain variation, range of effective bypass door operation, and level of the setpoint.

Although open-loop testing showed that control signal gain varied by as much as a factor of three over the range of throat Mach numbers considered, scheduling of gain with bypass door position was not required. Satisfactory closed-loop operation over the Mach number range from 0.9 to 1.5 was obtained using a constant electronic gain level in the outer loop.

The bypass door control response to engine weight flow transients was very satisfactory. Many of these transients were substantially faster than those expected in a full-scale intake, yet the pressure recovery at the compressor face was affected negligibly during each transient.

Data acquired from the many pulsator frequency sweep runs show good agreement with the mathematical model of the intake dynamics developed thus far. These data will aid in the further refinement of such analytic tools.

References

[1] Conners, J. F., "Some Aspects of Supersonic Inlet Stability," RM E55L16a, Oct. 1961, NASA.

[2] Willoh, Ross G., "A Mathematical Analysis of Supersonic Inlet Dynamics," TN D-4969, Dec. 1968, NASA.

DECEMBER 1971 J. AIRCRAFT VOL. 8, NO. 12

Wind-Tunnel Systems and Techniques for Aircraft/Stores Compatibility Studies

S. B. Moore
Vought Aeronautics Company, Dallas, Texas

A comprehensive presentation of advanced wind-tunnel techniques and facilities used in aircraft store carriage and delivery studies is presented. Extensive static stability, control, and metric store tests aid in predictions of aircraft performance and structural requirements. Investigations with scaled dynamic models are used to determine the flutter boundaries and aeroelastic effects caused by large store aerodynamic and inertia forces. Methods used to obtain mutual aerodynamic interference of wing-pylon-store combinations and external store aerodynamic interference on control surface effectiveness are described. State-of-the-art scaled dynamic separation and captive trajectory systems, their current and potential capabilities and limitations, are discussed. The quality of wind-tunnel simulation, in the general sense, is discussed and present limitations and potential improvements are pointed out.

Nomenclature

C_L = lift coefficient
E = modulus of elasticity
F = force
I = moment of inertia
L = lift, length
M = moment, Mach number, mass
P = load
PM = pitching moment
S = reference area, stress
V = velocity
W = weight
Z = linear displacement, vertical axis
$\dot{Z}$ = linear velocity
c = reference length, distance to neutral axis in bending
p = static pressure
q = dynamic pressure
x = longitudinal axis
y = lateral axis
z = vertical axis
λ = model scale, c_m/c_f
ρ = density
θ = pitch angle
$\dot{\theta}$ = angular velocity
β = yaw angle
ϕ = roll angle

Subscripts

b = bending, base
f = full scale
m = model
s = sting

Received February 16, 1971; revision received June 21, 1971.
Index category: Aircraft and Component Wind-Tunnel Testing.

* Engineering Specialist, Engineering Laboratories. Member AIAA.